Available online at www.sciencedirect.com
ScienceDirect
Journal of Sound and Vibration 299 (2007) 918–932
JOURNAL OF SOUND AND VIBRATION
www.elsevier.com/locate/jsvi

Forced vibro-acoustical analysis for a theoretical model of a passenger compartment with a trunk—Part II: Experimental part

Jin Woo Lee[a,*,1], Jang Moo Lee[b]

[a]*R&D Center, Digital Appliance Business, Samsung Electronics Co. Ltd., 416 Maetan-3-dong, Yeongtong-Gu, Suwon-City, Gyeonggi-Do 443-742, Republic of Korea*
[b]*School of Mechanical and Aerospace Engineering, Seoul National University, San 56-1, Shillim-dong, Kwanak-gu, Seoul 151-742, Republic of Korea*

Received 6 December 2005; received in revised form 2 May 2006; accepted 24 July 2006
Available online 17 October 2006

Abstract

In this paper, experimental investigation is carried out to validate the simulation results obtained by a new analytical model and the plane wave theory analysis, which were proposed in Part I of this work. In preliminary studies, the relation between a neck and a natural frequency is reviewed from a practical point of view, by using a second-order polynomial, for a coupled structural-acoustic system with the double cavities connected by a neck. The natural frequency increases with the neck's cross-sectional area, but the increasing rate decreases with the increasing cross-sectional area. On the contrary, it decreases as the neck approaches the corner from the center, but the decreasing rate increases around the corner. In acoustic experiments, the frequency response functions of two simplified rectangular double-cavity models and a half-scaled car model made out of Plexiglas are measured and compared for different cross-sectional areas and positions of a neck connecting two cavities. Experimental results qualitatively agreed well with the simulation results of Part I. The cavity-controlled mode of the coupled structural-acoustic system is more strongly affected by acoustical modification, which means the change in the neck's position and cross-sectional area considered in this paper, than by structural modification.

1. Introduction

In Part I of our work, a new theoretical model is proposed to investigate the effect of a neck (or a hole) of a package tray in a passenger compartment with a trunk on the acoustical properties of the vehicle. Analytical results obtained from case studies in Part I are qualitatively validated by experiments carried out in this paper

*Corresponding author. Tel.: +82 31 218 5205; fax: +82 31 218 5196.
E-mail address: jw062nam@yahoo.co.kr (J.W. Lee).
[1]Present address: National Creative Research Initiatives Center for Multiscale Design (311–206), School of Mechanical and Aerospace Engineering, Seoul National University, Seoul, 151–742, Republic of Korea.

0022-460X/$ - see front matter © 2006 Elsevier Ltd. All rights reserved.
doi:10.1016/j.jsv.2006.07.023

(Part II). The experimental results will not only conform the validity of the theoretical model but also provide insights on practical applications.

Many experimental investigations as well as theoretical simulation studies have been performed on simplified analytical models to explain and modify the dynamic characteristics of a real coupled structural-acoustic system [1,2]. Pan performed experiments for a rectangular panel-cavity system to verify the theoretical prediction that the modal decay time of sound waves in the enclosure depends upon the modal properties of the panel [3]. Trompette predicted the vibro-acoustical behavior of a structure by using his simplified techniques and adjusted the FE model to the experimental results on a metal box [4]. Kang introduced a simplified theoretical model and carried out experiments for a simplified compartment cavity model to investigate the coupling effects of the trim and air-gap on the frequency response characteristics of a passenger compartment [5]. Kim developed a computer program package for noise reduction of a vehicle and verified the effectiveness of the proposed method by means of experiment on a half-scaled car model [6]. Park studied the structural modification technique to reduce the vehicle noise and vibration and applied it to a half-scaled vehicle [7]. Nefske reviewed various techniques for structural-acoustic coupling analysis and experimentally verified them by applications to the production automobile [8].

Experimental modal techniques to extract acoustic modal properties of an acoustic cavity have been proposed. Nieter and Singh excited the acoustic system by a vibrating piston, which was driven by an electromagnetic shake [9]. For modal analysis, they determined the acoustic impedance of the system by using an accelerometer attached to the piston and a roving microphone at a number of locations. Kung and Singh advanced Nieter and Singh's acoustic modal analysis technique to identify modal parameters of a three-dimensional cavity [10]. They excited the cavity by a convertible acoustic driver and obtained acoustic transfer impedance for a number of cavity boundary locations enough to adequately describe all modes of interest. In our work, the acoustic system of interest is excited by a loudspeaker, and acoustic pressure is measured by a microphone, whose position is determined so that the peak frequencies related to the natural modes of interest are easy to find in the measured frequency response functions. Acoustic pressure distribution at each peak frequency is qualitatively conformed by using finite element analysis, which will not be illustrated in detail in this paper.

This paper experimentally investigates the acoustic response characteristics of the coupled structural-acoustic system with double cavities connected by a neck and qualitatively supports the validity of the simulation results of this system. First, the relation between a neck and a natural frequency is reviewed by using a simple polynomial, whose coefficients are determined by results obtained in the case studies in Part I. Second, in order to experimentally support the results obtained by using the new coupled structural-acoustic model and the proposed theoretical method, a simplified enclosure (double cavities connected by a neck) was made of Plexiglas. The relation between a neck (cross-sectional area or position) and measured natural frequencies is compared with that obtained from theoretical calculation. And then, the acoustic response of a half-scaled Plexiglas car was measured for different areas and positions of holes on the package tray. The experimental results will be explained by using the relation between the cross-sectional area and position of holes on the package tray and natural frequencies, which is obtained from simulation results. Also, the possibility that modifying position and cross-sectional area of holes on the package tray can change the acoustic characteristics of an automobile with a trunk will be addressed.

2. Review of results in case studies of part I

A low-order polynomial, which can express the relation between a neck's position or cross-sectional area and the natural frequencies of double cavities connected by a neck, is very crucial and useful to NVH engineers from a practical point of view. For this reason, the results in the case studies of the companion paper (Part I) are curve-fitted by using a second-order polynomial expressed by

$$\Omega_i = \beta_2\eta^2 + \beta_1\eta^1 + \beta_0, \tag{1}$$

where $\beta_i (i = 0, 1, 2)$ are coefficients, η is an independent variable expressing a neck's position or cross-sectional area, and Ω_i is the natural frequency. The coefficients β_i for a neck's position are determined by least-squares method in Matlab and displayed with correlation values (R^2) in Table 1, where the first three natural

Table 1
Coefficients and correlation value (R^2) for curve fits based on Eq. (1): a neck's position

	η	Neck's position (g_n/h_1)				Coefficients			Correlation value (R^2)
		0.0	0.3	0.6	0.9	β_0	β_1	β_2	
Case I-a	Ω_1	0.2259	0.2258	0.2257	0.2249	0.2259	0.0009	−0.0022	0.9882
	Ω_2	0.5877	0.5823	0.5661	0.4902	0.5868	0.0450	−0.1681	0.9970
	Ω_3	1.1589	1.1524	1.1297	1.0925	1.1590	0.0028	−0.0853	0.9999
Case I-b	Ω_1	0.5231	0.5209	0.5084	0.4629	0.5220	0.0439	−0.1203	0.9891
	Ω_2	0.6306	0.6271	0.6129	0.5909	0.6307	0.0018	−0.0514	0.9996
	Ω_3	1.1622	1.1557	1.1333	1.0969	1.1623	0.0020	−0.0831	0.9999
Case II-a	Ω_1	0.1928	0.1926	0.1915	0.1879	0.1927	0.0032	−0.0094	0.9917
	Ω_2	0.2529	0.2528	0.2526	0.2516	0.2529	0.0009	−0.0025	0.9770
	Ω_3	0.6193	0.6142	0.5902	0.5307	0.6185	0.0394	−0.1511	0.9972
Case II-b	Ω_1	0.4765	0.4741	0.4614	0.4220	0.4757	0.0338	−0.1028	0.9930
	Ω_2	0.5803	0.5802	0.5795	0.5777	0.5803	0.0014	−0.0047	0.9971
	Ω_3	0.6909	0.6880	0.6754	0.6508	0.6908	0.0100	−0.0603	0.9997

frequencies are used. Fig. 1 shows the natural frequency with a neck's position and its fitting curve, which is a parabolic curve that describes the right-hand side of a parabola bending down. Natural frequency decreases with a neck's position away from the center. It hardly decreases around the center, but dramatically decreases around the edge. Table 2 displays the coefficients of the relation equation and its correlation coefficients, which express the relation between a neck's cross-sectional area and a natural frequency. As shown in Fig. 2, the fitting curve describes the left-hand side of a parabola bending down, and it looks like a linear curve because its slope is very small in the third natural frequency. In general, natural frequency increases with a neck's cross-sectional area in the range selected in our simulation results, but the increasing rate decreases with increasing cross-sectional area.

The relation between a neck and natural frequencies in double cavities connected by a neck will be qualitatively investigated in the following experiment. The second-order polynomial expressed by Eq. (1) is applied to simplified experimental models to validate the simple relation equation. Two experimental models are used: double rectangular cavities connected by a neck (see Fig. 3(a)); and double rectangular cavities connected by a neck and blocked by a steel plate at one end (see Fig. 3(b)).

3. Acoustic response of simplified cavity models

3.1. Experimental setup

Fig. 3 shows two experimental models made out of 12 mm-thick Plexiglas. All surfaces of the two cavities in Fig. 3(a) are surrounded with Plexiglas plates, but one surface of cavity 2 in Fig. 3(b) is blocked by a clamped steel plate of 1.8 mm in thickness. Table 3 shows the values of the physical parameters of the experimental models. Between the two cavities, eight kinds of rectangular Plexiglas plates were installed to change the neck's cross-sectional area and its position. In the 1st experimental model (see Fig. 3(a)), a loudspeaker placed at the bottom of cavity 1 excited the enclosure and was controlled by the Dynamic Signal Analyzer (HP35670A), which produced a swept sine signal with a step of 0.50 Hz. To measure the input signal of the speaker, an accelerometer was attached to the center of the diaphragm of the speaker. The accelerometer was so light that its mass effect on the speaker's behavior could be ignored. In the second experimental model (see Fig. 3(b)), the external force by an impact hammer excited the acoustic field. In all of two experiments, two 1/2-in microphones (B&K 4190) were used to measure acoustic pressure in the enclosure: one was located at the corner of the bottom surface in cavity 1 and the other at the same position in cavity 2.

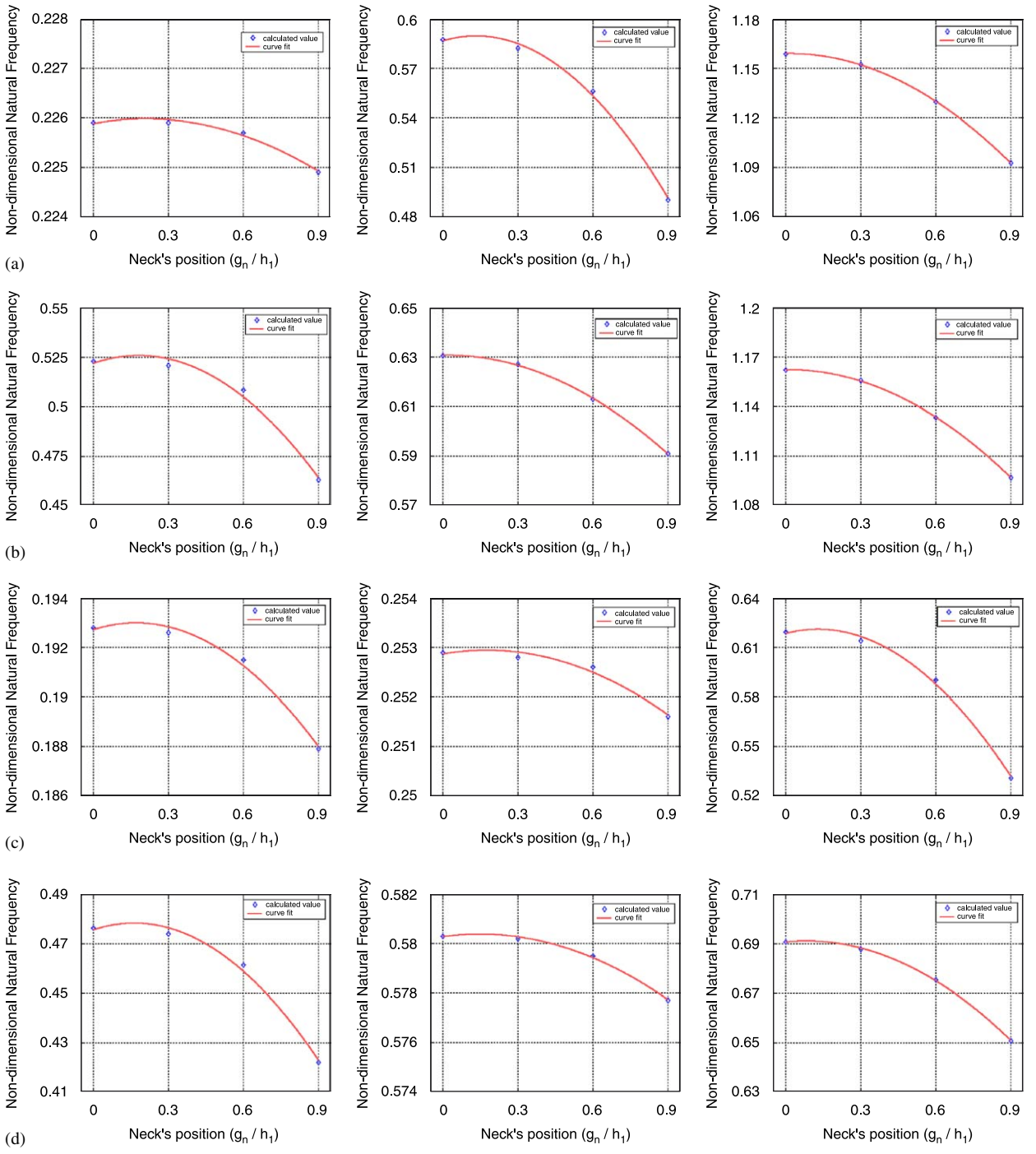

Fig. 1. Relation between a neck's position and natural frequencies of double cavities connected by a neck and blocked by a mechanical oscillator. (a) Case I-a, (b) Case I-b, (c) Case II-a and (d) Case II-b.

3.2. *Acoustic response of rectangular double cavities connected by a neck*

In order to investigate the effect of the cross-sectional area of a neck on acoustic natural frequencies, five kinds of Plexiglas plates were installed between cavities 1 and 2: a rectangular Plexiglas plate without a hole

Table 2
Coefficients and correlation value (R^2) for curve fits based on Eq. (1): a neck's cross-sectional area

	η	Neck's cross-sectional area ratio (h_n/h_1)					Coefficients			Correlation value (R^2)
		0.1	0.2	0.3	0.4	0.5	β_0	β_1	β_2	
Case I-a	Ω_1	0.2259	0.2263	0.2264	0.2266	0.2267	0.2256	0.0040	−0.0036	0.9764
	Ω_2	0.5877	0.6429	0.6772	0.7017	0.7198	0.5270	0.6830	−0.6000	0.9980
	Ω_3	1.1589	1.2173	1.2688	1.3170	1.3604	1.0970	0.6454	−0.2379	1.0000
Case I-b	Ω_1	0.5231	0.5391	0.5448	0.5478	0.5496	0.5068	0.1950	−0.2221	0.9808
	Ω_2	0.6306	0.6709	0.7002	0.7223	0.7388	0.5848	0.5027	−0.3914	0.9996
	Ω_3	1.1622	1.2198	1.2709	1.3188	1.3621	1.1012	0.6351	−0.2271	1.000
Case II-a	Ω_1	0.1928	0.1947	0.1957	0.1964	0.1969	0.1908	0.0232	−0.0221	0.9950
	Ω_2	0.2529	0.2534	0.2537	0.2539	0.2541	0.2524	0.0059	−0.0050	0.9955
	Ω_3	0.6193	0.6698	0.7010	0.7234	0.7398	0.5638	0.6246	−0.5500	0.9980
Case II-b	Ω_1	0.4765	0.4980	0.5086	0.5150	0.5193	0.4534	0.2680	−0.2757	0.9931
	Ω_2	0.5803	0.5817	0.5825	0.5832	0.5836	0.5788	0.0171	−0.0150	0.9977
	Ω_3	0.6909	0.7222	0.7442	0.7611	0.7738	0.6559	0.3860	−0.3021	0.9994

and four rectangular Plexiglas plates with a square hole at the center. Fig. 4 displays the measured frequency response functions for different cross-sectional areas of a square hole, whose sides are 0, 40, 80, 120 and 160 mm. In each frequency response function, the input signal represented the acceleration of the speaker and the response signal represented the acoustic pressure measured at microphone 1. As predicted in Ref. [11], the neck's cross-sectional area strongly affected the x-axial modes but hardly affected the y-axial modes around 260 Hz. Table 4 summarizes the non-dimensional natural frequencies for a neck's cross-sectional area, coefficients and correlation values of curve fits based on Eq. (1) for the first two modes (x-axial modes). Considering the correlation values, the relation equation (Eq. (1)) well represents the change in natural frequency by the cross-sectional area. The changing trend is very similar to the simulation results (see Fig. 5).

Fig. 6 displays the frequency response functions measured at microphone 2 for three positions of the neck: center $(1, 0, 0)$; middle $(1, 0.135, 0.085)$; and corner $(1, 0.27, 0.17)$ (see Fig. 3). Similar to the results in the preceding experiment, x-axial modes were only affected by the neck's position. Non-dimensional natural frequencies according to a neck's position, coefficients and correlation values of curve fits based on Eq. (1) for two x-axial modes are summarized in Table 5. The curve fits, as shown in Fig. 7, describe the right-hand side of a parabola bending down as predicted in the simulation results. Natural frequencies of x-axial modes (the first and second modes) decrease as the square hole approaches the corner. Also, the decreasing rate was larger in the 1st mode than in the 2nd mode.

In comparison of the natural frequencies for different cross-sectional areas and positions of the neck, the first two natural frequencies were lower for a hole of 100 mm × 100 m at the corner than for a hole of 80 mm × 80 mm at the center: $0.2768 < 0.3023$; and $1.0198 < 1.0282$. This result means that the amount of increase in natural frequency due to cross-sectional area is less than amount of decrease due to position shift. And it implies that position and cross-sectional area of necks can be properly adjusted to obtain desirable acoustic characteristics.

3.3. Acoustic response for double rectangular cavities connected by a neck and blocked by a steel plate at one end

In the preliminary experiment, impact hammer test was carried out to identify the modal characteristics of the clamped steel plate. An accelerometer was fixed at the point of 21, and exciting force was applied to 48 points in order by an impact hammer. An input signal and a response signal were measured by using a force transducer and an accelerometer, respectively. With 48 frequency response functions, modal analysis was done by using Cada-X 3.5. Natural modes of the clamped plate are displayed in Fig. 8.

When an external force was applied to point 21 on the clamped plate, acoustic pressure in the coupled system was measured for seven different Plexiglas plates installed between two cavities in order to obtain resonance frequencies depending on change in the cross-sectional area and position of a square hole: the sides

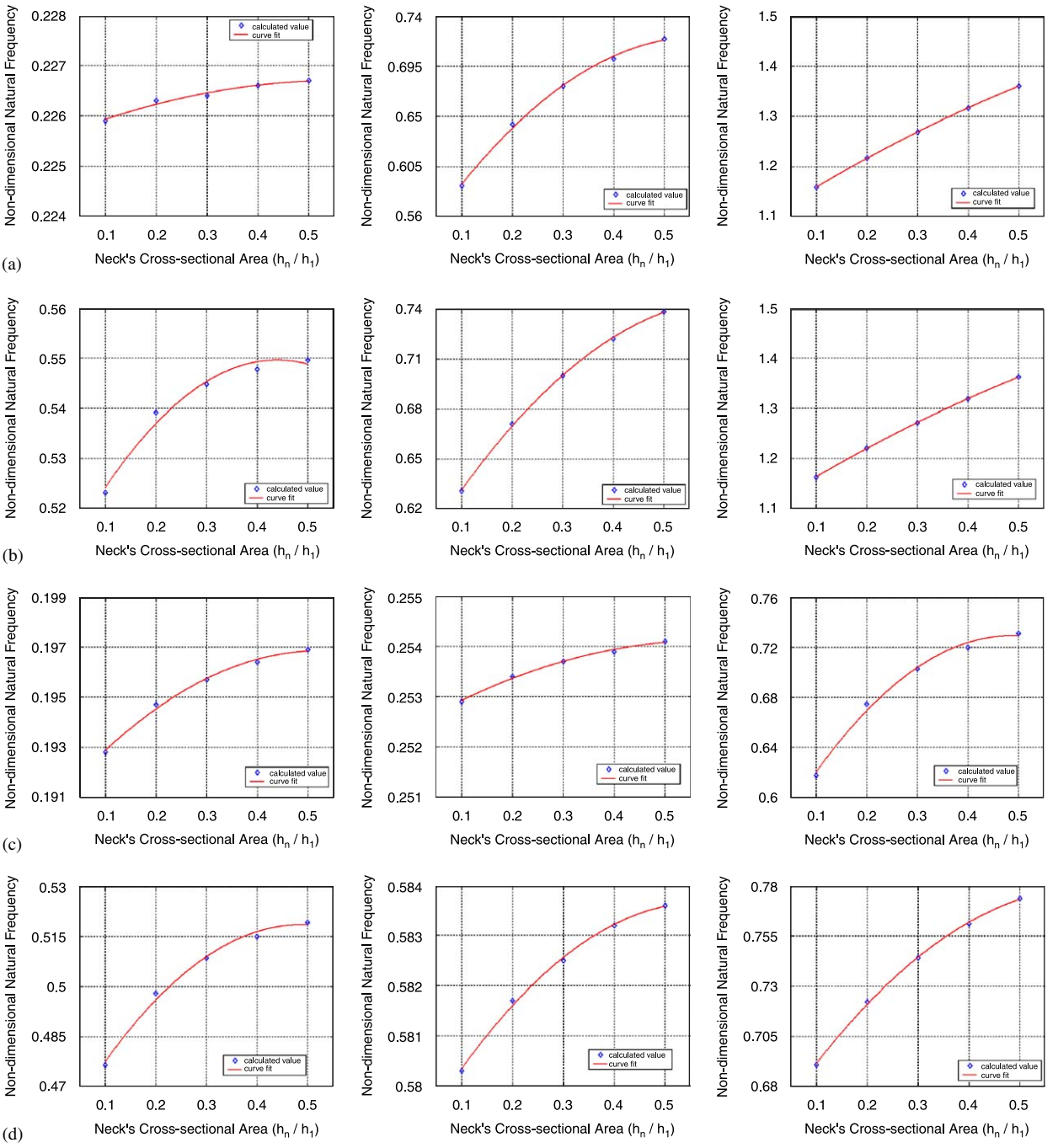

Fig. 2. Relation between a neck's cross-sectional area and natural frequencies of double cavities connected by a neck and blocked by a mechanical oscillator. (a) Case I-a, (b) Case I-b, (c) Case II-a and (d) Case II-b.

of the hole are the same those in Table 3. Fig. 9 shows the frequency response functions with the cross-sectional area of a hole. In each frequency response function, a force transducer attached to the impact hammer measured an input signal, and acoustic pressure measured at microphone 1 was used as a response signal. In the frequency range of 180–200 Hz and of 30–50 Hz, natural frequencies of cavity-controlled modes increased with cross-sectional area of a hole. Table 6 summarizes the non-dimensional natural frequencies of

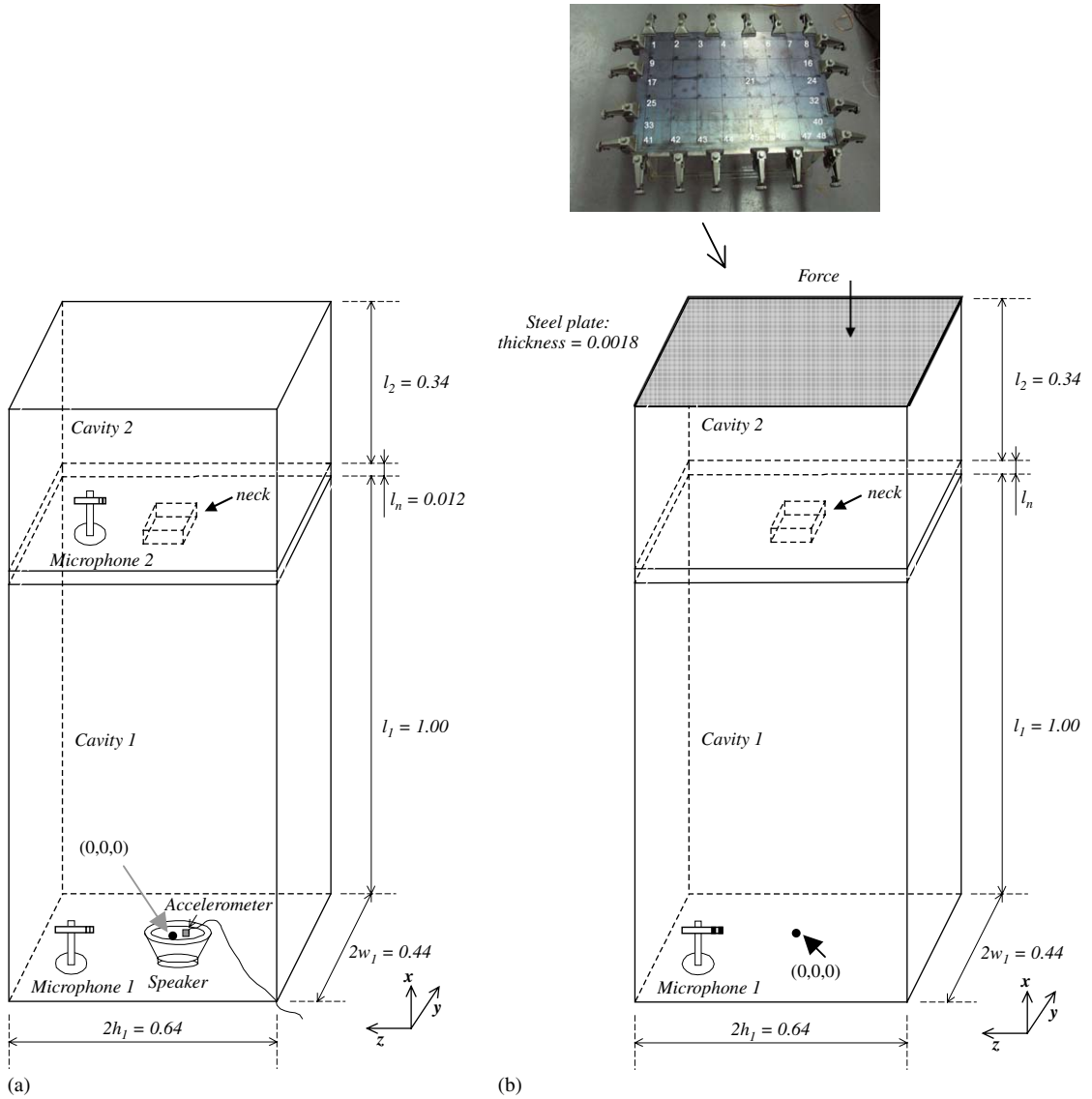

Fig. 3. Experimental setup to investigate a neck's effect on natural frequency of double cavities. (a) 1st simplified experimental model and (b) 2nd simplified experimental model.

Table 3
Value of physical parameters of simplified experimental models

	Cavity 1	Cavity 2	Neck							
			Effect of cross-sectional area					Effect of position		
Length (m)	1.000	0.340	0.012	0.012	0.012	0.012	0.012	0.012	0.012	0.012
Width (m)	0.440	0.440	0	0.040	0.080	0.120	0.160	0.100	0.100	0.100
Height (m)	0.640	0.640	0	0.040	0.080	0.120	0.160	0.100	0.100	0.100
Position	—	—	—	Center	Center	Center	Center	Center	Middle	Corner
Cross-sectional area	0.2816	0.2816	0	0.0016	0.0064	0.0144	0.0256	0.0100	0.0100	0.0100

Neck's position: center (1, 0, 0), middle (1, 0.135, 0.085), corner (1, 0.27, 0.17).

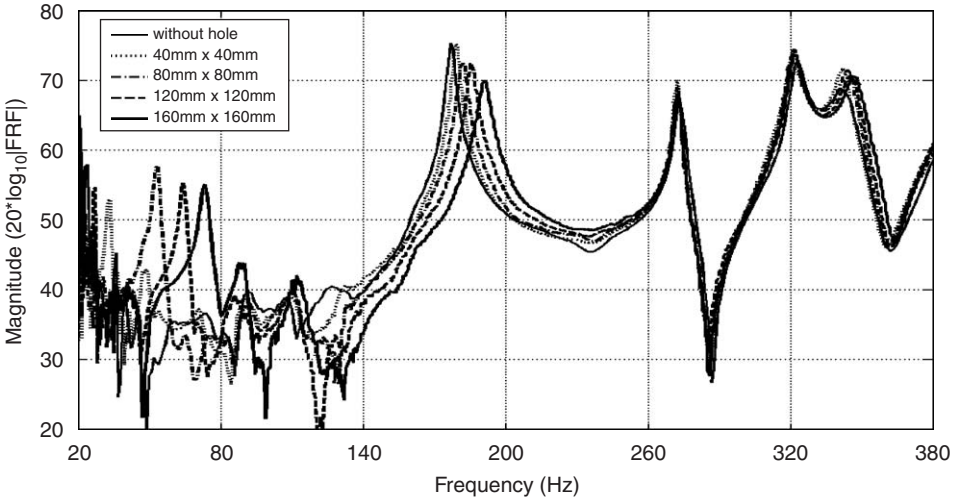

Fig. 4. Frequency response functions of the 1st simplified experimental model measured at microphone 1 with a cross-sectional area of a neck changing.

Table 4
Natural frequencies of the 1st simplified experimental model with change in a neck's cross-sectional area, coefficients and correlation value (R^2) for curve fits based on Eq. (1)

	η	Neck's cross-sectional area ratio (S_n/S_1)				Coefficients			Correlation value (R^2)
		0.0057	0.0227	0.0511	0.0909	β_0	β_1	β_2	
x-axial mode	Ω_1	0.1893	0.3023	0.3616	0.4153	0.1677	5.7959	−34.152	0.9749
x-axial mode	Ω_2	1.0113	1.0282	1.0480	1.0791	1.0073	0.8588	−0.7955	0.9979
y-axial mode	Ω_3	1.5395	1.5367	1.5367	1.5395	—	—	—	—
x-y tangential mode	Ω_4	1.8164	1.8136	1.8136	1.8249	—	—	—	—

Ω_i is non-dimensional natural frequency, which is a measured peak frequency divided by the 1st natural frequency (177 Hz) of cavity 1.

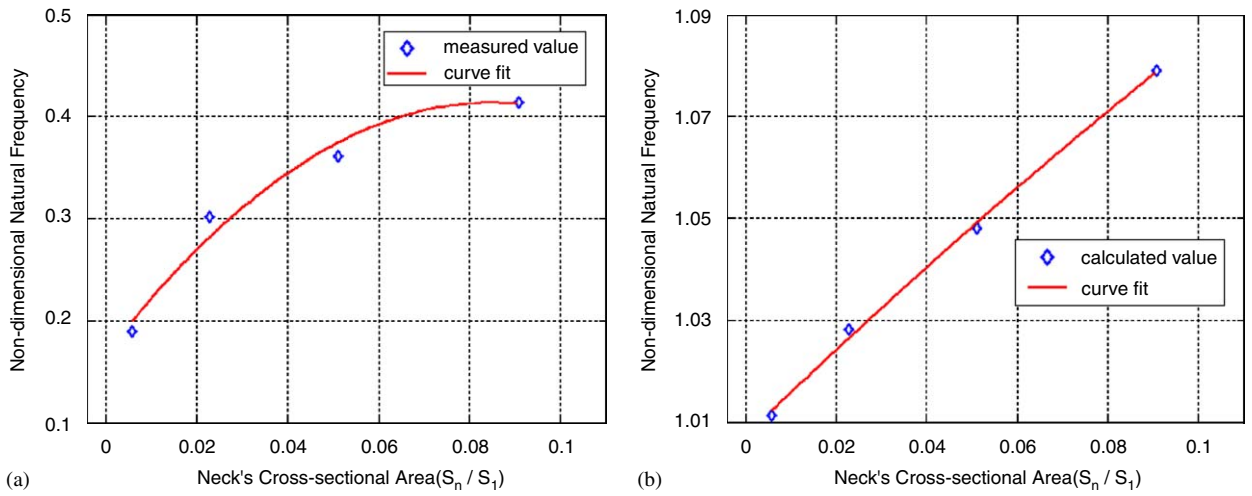

Fig. 5. Relation between a neck's cross-sectional area and natural frequencies of the 1st simplified experimental model. (a) 1st cavity-controlled mode and (b) 2nd cavity-controlled mode.

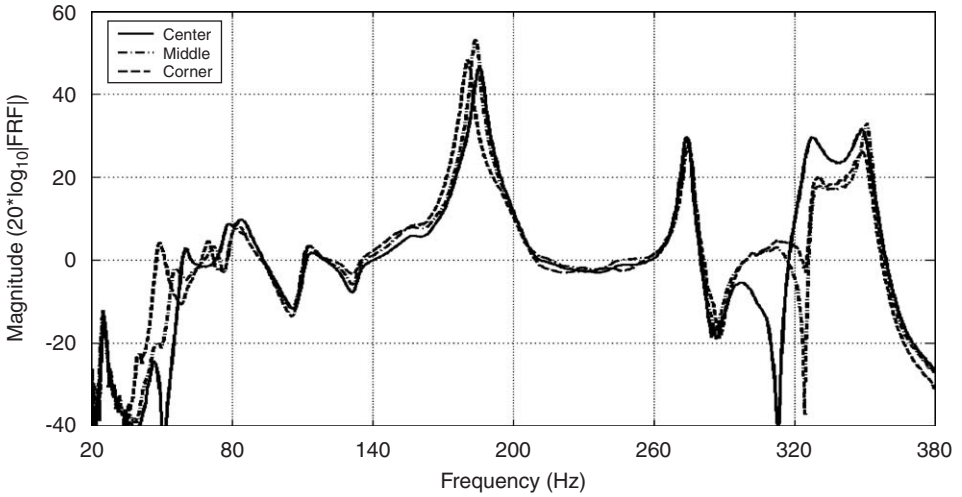

Fig. 6. Frequency response functions of the 1st simplified experimental model measured at the microphone 2 with the position of a neck.

Table 5
Natural frequencies of the 1st simplified experimental model with a neck's position, coefficients and correlation value (R^2) for curve fits based on Eq. (1)

	η	Neck's position			Coefficients			Correlation value (R^2)
		Center	Middle	Corner	β_0	β_1	β_2	
x-axial mode	Ω_1	0.3418	0.3164	0.2768	0.3418	−0.0896	−0.1681	1.000
x-axial mode	Ω_2	1.0508	1.0395	1.0198	1.0508	−0.0345	−0.1008	1.000
y-axial mode	Ω_3	1.5452	1.5452	1.5452	—	—	—	—
x-y tangential mode	Ω_4	1.8249	1.8249	1.8362	—	—	—	—

Ω_i is non-dimensional natural frequency, which is a measured peak frequency divided by the 1st natural frequency (177 Hz) of cavity 1.

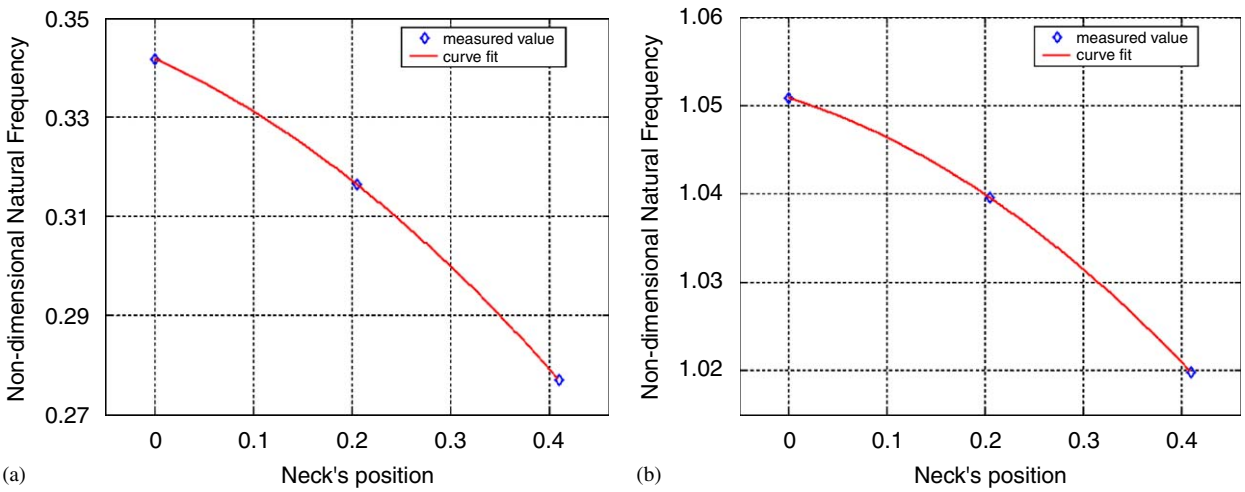

Fig. 7. Relation between a neck's position and natural frequencies of the 1st simplified experimental model. (a) 1st cavity-controlled mode and (b) 2nd cavity-controlled mode.

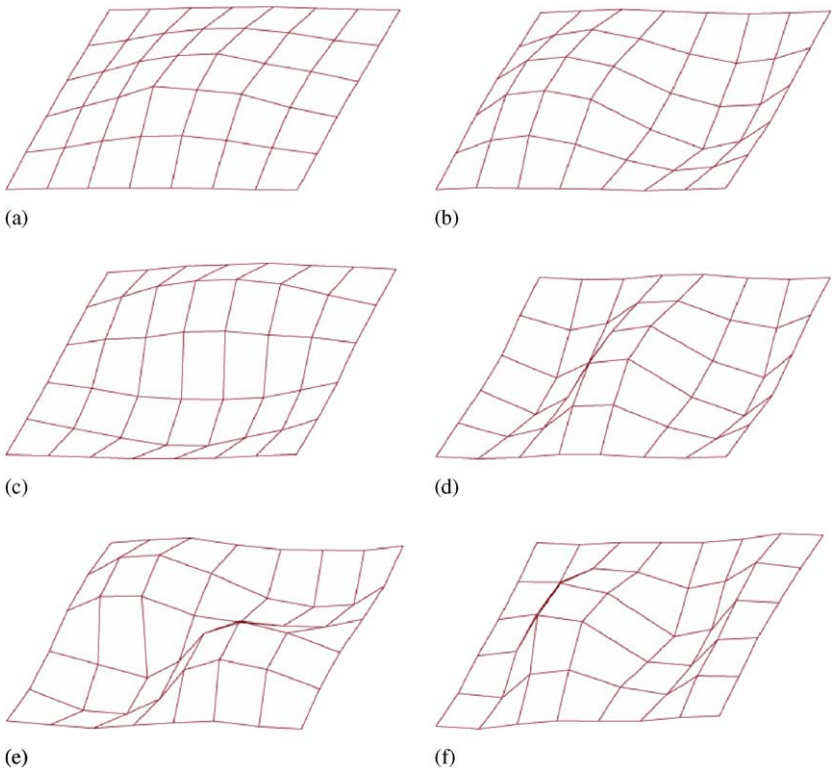

Fig. 8. Natural modes of the clamped plate. (a) 1st natural mode (52.44 Hz), (b) 2nd natural mode (69.12 Hz), (c) 3rd natural mode (98.86 Hz) (d) 4th natural mode (110.75 Hz), (e) 5th natural mode (141.48 Hz) and (f) 6th natural mode (153.17 Hz).

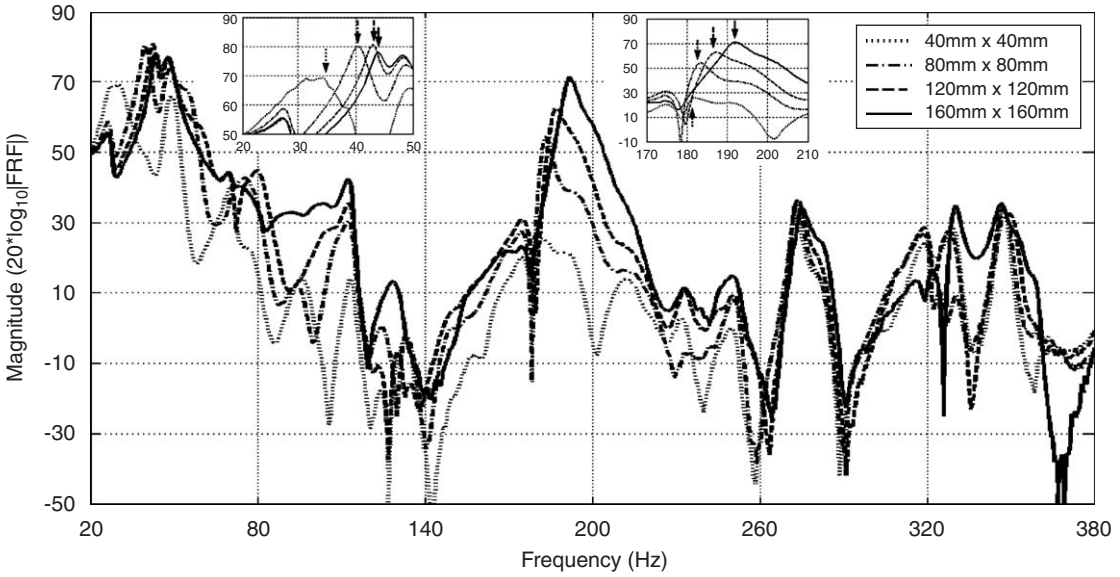

Fig. 9. Frequency response functions of the 2nd simplified experimental model measured at the microphone 1 with a cross-sectional area of a square hole changing.

the 2nd experimental model with a neck's cross-sectional area, coefficients and correlation values of curve fits based on Eq. (1) for two cavity-controlled modes. Also, Fig. 10 shows the curve fits that describe the left-hand side of a parabola bending down like those obtained in the preceding experiment. Fig. 11 shows the frequency

Table 6
Natural frequencies of the 2nd simplified experimental model with change in a neck's cross-sectional area, coefficients and correlation value (R^2) for curve fits based on Eq. (1)

	η	Neck's cross-sectional area ratio (S_n/S_1)				Coefficients			Correlation value (R^2)
		0.0057	0.0227	0.0511	0.0909	β_0	β_1	β_2	
x-axial mode	Ω_1	0.2090	0.2260	0.2401	0.2458	0.2038	1.0689	−6.7085	0.9964
x-axial mode	Ω_2	1.0226	1.0367	1.0565	1.0847	1.0185	0.7827	−0.6099	0.9996

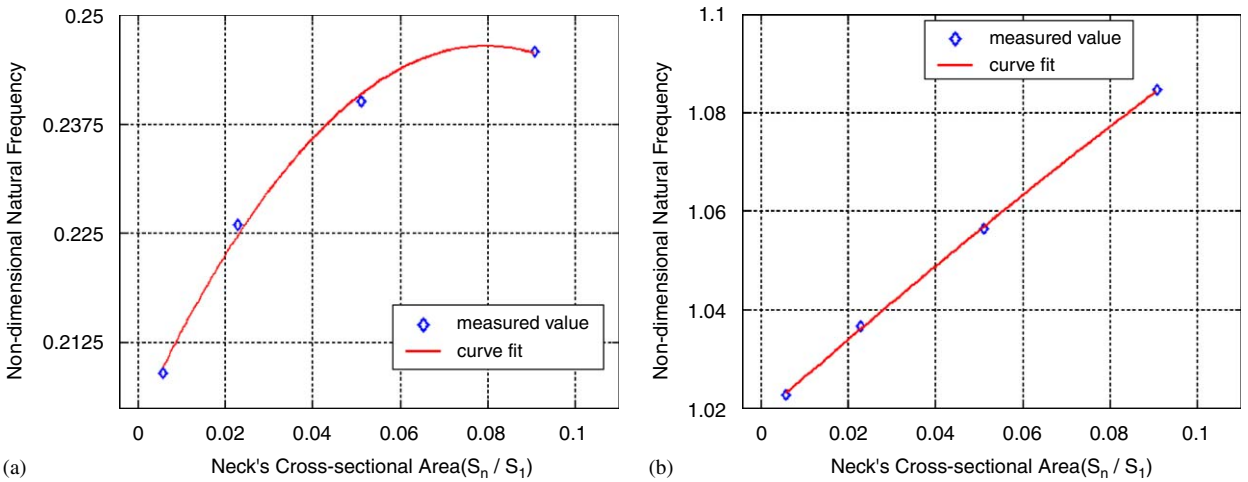

Fig. 10. Relation between a neck's cross-sectional area and natural frequencies of the 2nd simplified experimental model. (a) 1st cavity-controlled mode and (b) 2nd cavity-controlled mode.

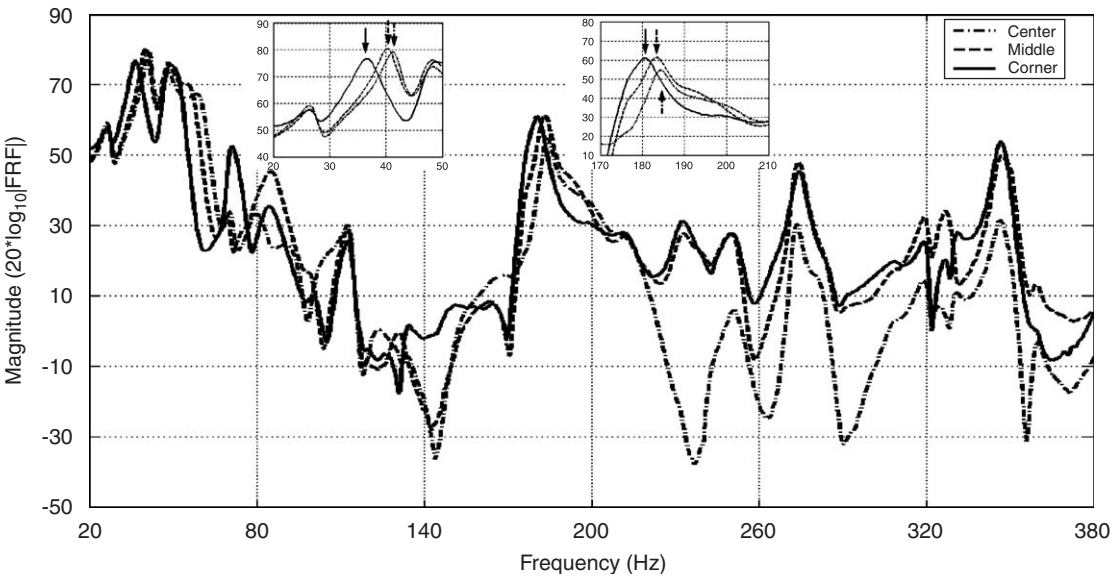

Fig. 11. Frequency response functions of the 2nd simplified experimental model measured at microphone 1 with position of a square hole changing.

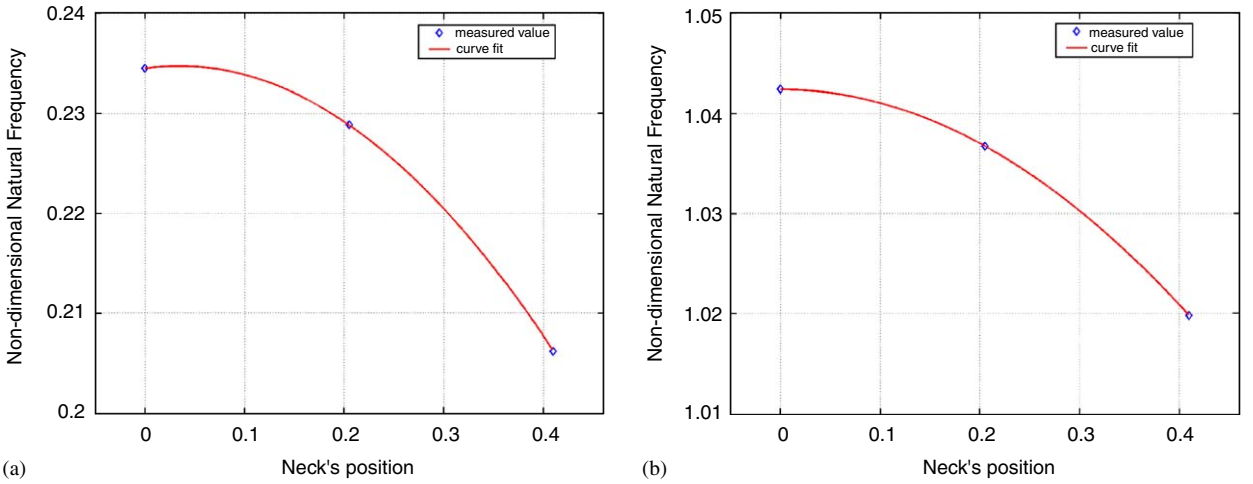

Fig. 12. Relation between a neck's position area and natural frequencies of the 2nd simplified experimental model. (a) 1st cavity-controlled mode and (b) 2nd cavity-controlled mode.

Table 7
Natural frequencies of the 2nd simplified experimental model with change in a neck's position, coefficients and correlation value (R^2) for curve fits based on Eq. (1)

Cavity-controlled mode	η	Neck's position			Coefficients			Correlation value (R^2)
		Center	Middle	Corner	β_0	β_1	β_2	
x-axial mode	Ω_1	0.2345	0.2888	0.2062	0.2345	0.0138	−0.2017	1.000
x-axial mode	Ω_2	1.0424	1.0367	1.0198	1.0424	0.000.0	−0.1345	1.000

response functions measured at microphone 1 by an external force applied to the point 21 for three different positions of a square hole. As a hole approached the corner, resonance frequencies of cavity-controlled modes decreased. These trends correspond to that obtained from the simulation results. Fig. 12 displays non-dimensional natural frequencies measured for three different positions of a hole and their curve fits with coefficients and correlation values of the relation equation, which are summarized in Table 7. The curve fits describe the right-hand side of a parabola bending down as shown in the results of the preceding experiment.

4. Acoustic response of a half-scaled car

In order to increase the validity of the results obtained from simulation studies (Part I) and the simplified experimental models, a simplified car with a trunk made of Plexiglas was constructed as shown in Fig. 13. Since the dimensions of the simplified car are approximately half of those of a real car, this car is called a half-scaled car. Positions and cross-sectional areas of holes in the Plexiglas package tray shown in Fig. 14 were determined on the basis of those of a package tray in a real sedan with a trunk: two speaker holes (cross-sectional area = 3273 mm^2); 11 air ventilation holes (cross-sectional area = 5775 mm^2); and two holes for electric devices (cross-sectional area = 9638 mm^2).

Frequency response functions were measured for four cases shown in Table 8: In case A, only two holes for electric devices were open but the other holes were closed; in case B, only air ventilation holes were open; in case C, only two speaker holes were open; and in case D, all holes were open. In each test, the acoustic cavity was excited by a loudspeaker, which was located at the right-hand side of the footwell. The loudspeaker produced a swept sine signal with a step of 0.5 Hz, which was controlled by the Dynamic Signal Analyzer (HP35670A). A small accelerometer was attached to the center of the diaphragm to measure the input signal

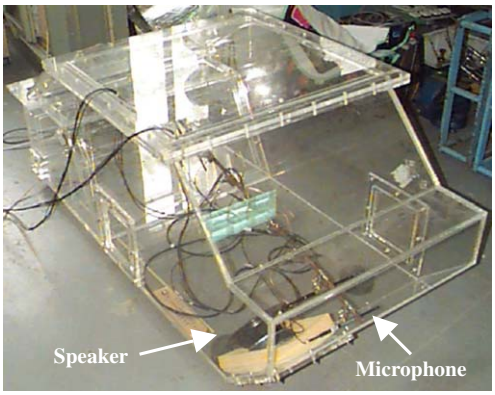

(a)

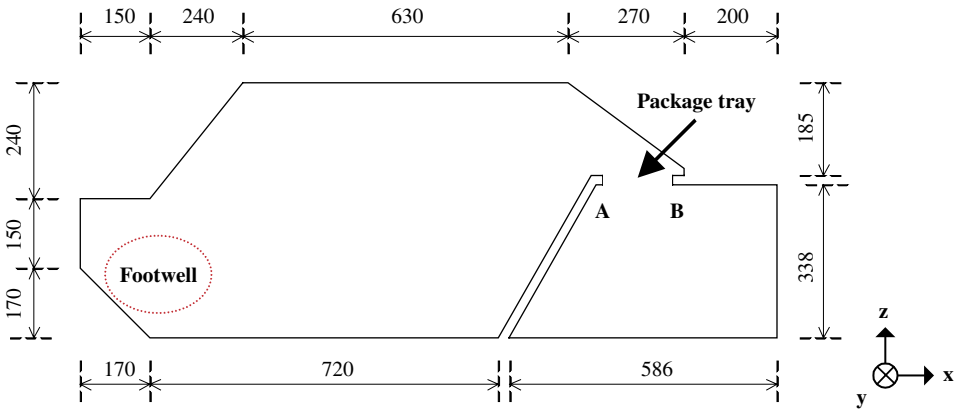

(b) Width: 680 Unit: mm

Fig. 13. A half-scaled car made of Plexiglas of 12 mm thickness. (a) A half-scaled Plexiglas car and (b) Dimensions of a half-scaled car.

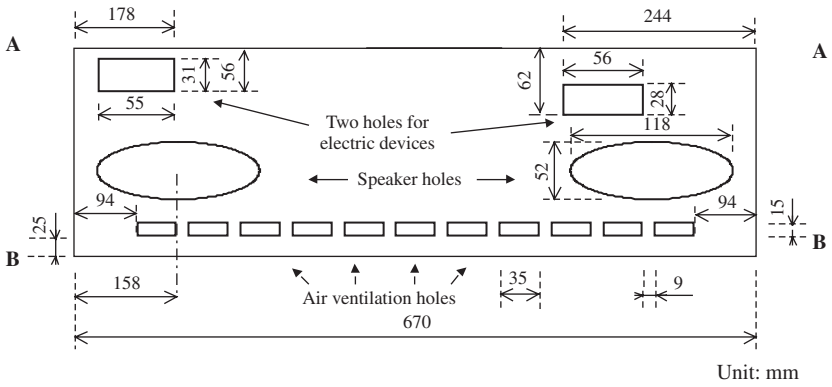

Fig. 14. A simplified package tray: dimensions and positions of holes.

of the speaker. And acoustic pressure was measured by using a microphone (1/2 in condenser microphone—B&K 4190) at the left-hand side of the footwell and used as the response signal.

Fig. 15 compares four frequency response functions of the half-scaled Plexiglas car for the four cases. The peaks in the frequency range of 40–90 Hz indicate the first longitudinal mode, which would not exist without a trunk cavity. And the peaks around 190 Hz represent the second longitudinal mode, whose natural frequency

Table 8
Cross-sectional areas (unit: mm^2) and natural frequency (unit: Hz) for four cases in the package tray of a half-scaled car

	Case A	Case B	Case C	Case D	Cross-sectional area
Holes for electric devices	Opening	Closing	Closing	Opening	3273
Holes for air ventilation	Closing	Opening	Closing	Opening	5775
Speaker holes	Closing	Closing	Opening	Opening	9638
Total cross-sectional area of opening holes	3273	5775	9638	18686	—
1st natural frequency	46.0 Hz	54.5 Hz	58.5 Hz	70.5 Hz	—
2nd natural frequency	184.0 Hz	187.0 Hz	187.5 Hz	195.0 Hz	—

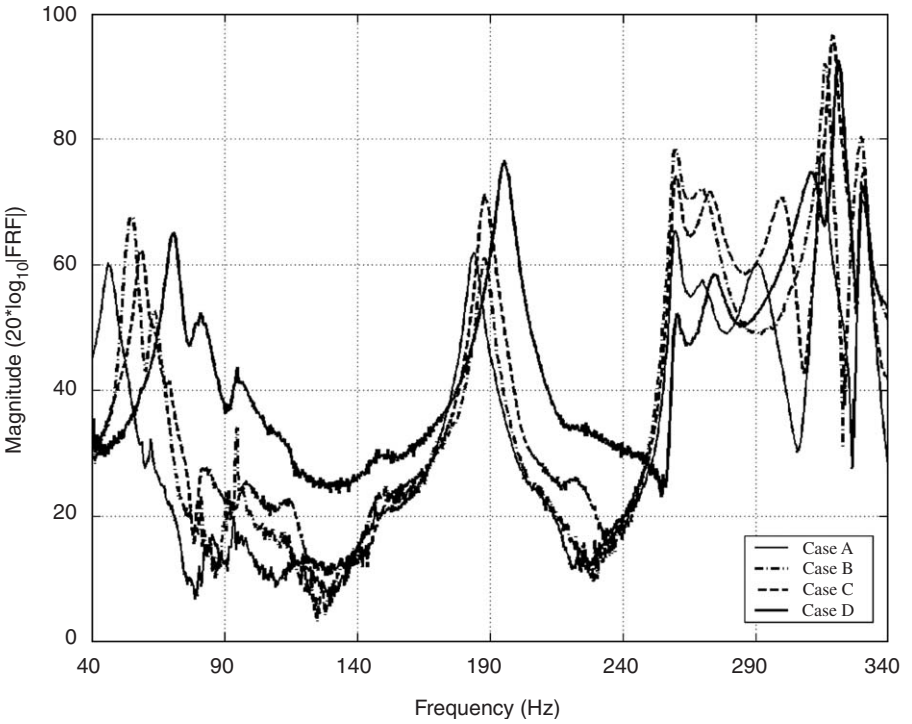

Fig. 15. Frequency response functions at the right-hand side of the footwell with cross-sectional area of opening holes on the package tray. Total cross-sectional area of opening holes: case A = 3273 mm^2; case B = 5775 mm^2; case C = 9638.4 mm^2; and case D = 18686 mm^2.

changes due to a trunk cavity and holes on the package tray. The third natural frequency around 260 Hz hardly changes because the associated natural mode has acoustic pressure distribution only in the y-axis. As shown in Table 8, the first two natural frequencies increase with the cross-sectional area of opened holes, but the increasing rate is not proportional to the increasing cross-sectional area. The cross-sectional area of case C is 1.7 times larger than that of case B, but the natural frequency difference is much smaller than the results of the other cases. This result implies that the position of holes as well as the cross-sectional area of holes affects the acoustic coupling between two cavities as proved in the simulation results and experimental results for simplified models. While holes for air ventilation were evenly distributed from center to both corners, two speaker holes were located around the corner. That is, the associated natural frequency in case C increased due to the increasing cross-sectional area but decreased due to the increasing effective length of holes. Considering that the first two natural modes have the high possibility of generating booming noise in a sedan with a trunk, related natural frequencies could be tuned by adjusting the cross-sectional area and position of holes on the package tray between the passenger compartment cavity and the trunk cavity.

5. Conclusions

In this paper, results obtained in the companion paper (Part I) were reviewed from a practical point of view, and acoustic experiment was carried out in order to qualitatively support the simulation results of a coupled structural-acoustic system with double cavities connected by a neck. A second-order polynomial was introduced to express the relation between a neck's position or cross-sectional area and the natural frequency of a coupled system. And the effect of a neck on natural frequency was experimentally investigated for two simplified experimental models and a half-scaled Plexiglas car. The relation between a natural frequency and a neck (cross-sectional area or position) was fitted by the parabolic curve bending down. The natural frequency increased with the neck's cross-sectional area, but its increasing rate decreased with the increasing cross-sectional area. However, it decreased but its decreasing rate increased, as the neck approached the corner from the center. In the acoustic experiment, only the natural frequencies of cavity-controlled modes, which were also longitudinal acoustic modes, were affected by the neck's characteristics, and the changing trend in the natural frequencies well agreed with the simulation results. And experimental results of the half-scaled car indicated that acoustic characteristics could be tuned by adjusting the position and cross-sectional area of the holes on the package tray of a sedan with a trunk.

Acknowledgment

This work was supported by the Brain Korea 21 project in 2005.

References

[1] L. Cremer, M. Heckl, *Structure-borne Sound: Structure Vibrations and Sound Radiation at Audio Frequencies*, Springer-Verlag, New York, 1972.
[2] L.E. Kinsler, A.R. Frey, A.B. Coppens, J.V. Sanders, *Fundamentals of Acoustics*, Wiley, New York, 1982.
[3] J. Pan, D.A. Bies, The effect of fluid-structural coupling on sound waves in an enclosure-Experimental part, *Journal of the Acoustical Society of America* 87 (2) (1990) 708–717.
[4] N. Trompette, M. Guerich, An experimental validation of vibro-acoustic prediction by the use of simplified methods, *Applied Acoustics* 66 (2005) 427–445.
[5] S.W. Kang, J.M. Lee, S.H. Kim, Structural-acoustic coupling analysis of the vehicle passenger compartment with the roof, air-gap, and trim boundary, *Journal of Vibration and Acoustics ASME* 122 (2000) 196–202.
[6] S.H. Kim, J.M. Lee, Practical method for noise reduction in a vehicle passenger compartment, *Journal of Vibration and Acoustics* 120 (1998) 199–205.
[7] Y.H. Park, Y.S. Park, Vehicle interior noise and vibration reduction using experimental structural dynamics modification, *SAE* 971915 (1997) 365–371.
[8] D.J. Nefske, J.A. Wolf Jr., L.J. Howell, Structural-acoustic finite element analysis of the automobile passenger compartment: a review of current practice, *Journal of Sound and Vibration* 80 (2) (1982) 247–266.
[9] J.J. Nieter, R. Singh, Acoustic modal analysis experiment, *Journal of the Acoustical Society of America* 72 (2) (1982) 319–326.
[10] C.H. Kung, R. Singh, Experimental modal analysis technique for three-dimensional acoustic cavities, *Journal of the Acoustical Society of America* 77 (2) (1985) 731–738.
[11] J.W. Lee, J.M. Lee, S.H. Kim, Acoustical analysis of multiple cavities connected by necks in series with a consideration of evanescent waves, *Journal of Sound and Vibration* 273 (2004) 515–542.